

Pandemic pharmaceutical dosing effects on wastewater treatment: no adaptation of activated sludge bacteria to degrade the antiviral drug Oseltamivir (Tamiflu[®]) and loss of nutrient removal performance

Frances R. Slater¹, Andrew C. Singer², Susan Turner³, Jeremy J. Barr¹ & Philip L. Bond¹

¹Advanced Water Management Centre (AWMC), The University of Queensland, St. Lucia, Qld, Australia; ²The Centre for Ecology and Hydrology, Wallingford, UK; and ³School of Biological Sciences, The University of Auckland, Auckland, New Zealand

Correspondence: Philip L. Bond, Gehrmann Laboratories, Advanced Water Management Centre (AWMC), The University of Queensland, Level 6, Research Road, St. Lucia, Qld 4072, Australia. Tel.: +61 7 334 63226; fax: +61 7 336 54726; e-mail: phil.bond@awmc.uq.edu.au

Received 31 August 2010; revised 28 October 2010; accepted 13 November 2010.
Final version published online 6 December 2010.

DOI:10.1111/j.1574-6968.2010.02163.x

Editor: Gilbert Shama

Keywords

antiviral degradation; pharmaceutical ecotoxicity; enhanced biological phosphorus removal (EBPR).

Abstract

The 2009–2010 influenza pandemic saw many people treated with antivirals and antibiotics. High proportions of both classes of drugs are excreted and enter wastewater treatment plants (WWTPs) in biologically active forms. To date, there has been no study into the potential for influenza pandemic-scale pharmaceutical use to disrupt WWTP function. Furthermore, there is currently little indication as to whether WWTP microbial consortia can degrade antiviral neuraminidase inhibitors when exposed to pandemic-scale doses. In this study, we exposed an aerobic granular sludge sequencing batch reactor, operated for enhanced biological phosphorus removal (EBPR), to a simulated influenza-pandemic dosing of antibiotics and antivirals for 8 weeks. We monitored the removal of the active form of Tamiflu[®], oseltamivir carboxylate (OC), bacterial community structure, granule structure and changes in EBPR and nitrification performance. There was little removal of OC by sludge and no evidence that the activated sludge community adapted to degrade OC. There was evidence of changes to the bacterial community structure and disruption to EBPR and nitrification during and after high-OC dosing. This work highlights the potential for the antiviral contamination of receiving waters and indicates the risk of destabilizing WWTP microbial consortia as a result of high concentrations of bioactive pharmaceuticals during an influenza pandemic.

Introduction

Society has never been more prepared for the emergence of pandemic influenza than at present, due in part to the development and stockpiling of a novel class of antiviral drugs, neuraminidase inhibitors, notably: Tamiflu[®] [oseltamivir ethylester-phosphate (OP)] and Relenza[®] (zanamivir). National stockpiling of neuraminidase inhibitors began in earnest with the emergence of the 2009 influenza pandemic (H1N1). These stockpiles were dominated by Tamiflu[®] largely owing to its relative ease of administration (tablet), as compared with Relenza (disc inhaler). Tamiflu[®] is a prodrug, which, after absorption into the blood, is converted to the active antiviral, oseltamivir carboxylate (OC), in the liver. Approximately 80% of an oral dose of

Tamiflu[®] is excreted as OC in the urine (He *et al.*, 1999), with the remainder excreted as OP in the faeces. Both the parent chemical and its bioactive metabolite ultimately reach the receiving wastewater treatment plants (WWTPs), where it was projected to reach a mean of ~2–12 µg L⁻¹ during a moderate and severe pandemic, respectively (A.C. Singer *et al.*, unpublished data).

Current evidence suggests conservation of OC as it passes through WWTPs (Fick *et al.*, 2007; Accinelli *et al.*, 2010; Ghosh *et al.*, 2010; Prasse *et al.*, 2010; Soderstrom *et al.*, 2010); hence, rivers receiving WWTP effluent will also be exposed to OC throughout a pandemic. Concentrations of between 293 and 480 ng OCL⁻¹ have been recorded in rivers receiving WWTP effluent during the 2009 pandemic (Ghosh *et al.*, 2010; Soderstrom *et al.*, 2010). Several studies have

demonstrated the potential for the removal of OC from freshwater (amended in some cases with sediment) and activated sludge (amended in some cases with a granular bioplastic formulation entrapping propagules of white rot fungi) via adsorption, microbial degradation and indirect photolysis (Accinelli *et al.*, 2007, 2010; Bartels & von Tumpling, 2008; Sacca *et al.*, 2009). A key factor in determining the amount of OC removal appears to be the length of incubation, with batch incubations of 40 days resulting in the degradation of up to 76% OC in the presence of an activated sludge inoculum (Accinelli *et al.*, 2010). However, batch experiments do not reflect the activities of a WWTP as the hydraulic residence time (HRT) for wastewater in the activated sludge system is commonly only a few hours and degradation would therefore be expected to be much lower. In a pandemic scenario, Tamiflu[®] use would rapidly increase over an 8-week period as the outbreak spread and would follow a similarly rapid decline after the peak (Singer *et al.*, 2007, 2008, unpublished data). We hypothesize that the prolonged exposure of WWTP microbial consortia over the course of a pandemic might hasten the generation of OC degraders in the activated sludge bacterial community, thereby minimizing the risks posed from widespread environmental release.

The key processes in WWTPs [removal of organic carbon, nitrogen (N) and phosphorus (P)] are microbiologically mediated by activated sludge. Activated sludge systems are constantly exposed to pharmaceuticals from a variety of sources (Daughton & Ternes, 1999); however, their effective toxicity remains unclear (i.e. impact on nutrient removal performance). The functioning of activated sludge under a pandemic scenario is of concern, given the projected heavy usage of not only antivirals but also antibiotics (Singer *et al.*, 2008, unpublished data). There is recent evidence that bacterial neuraminidases are important in biofilm formation (Soong *et al.*, 2006; Parker *et al.*, 2009). Consequently, antiviral neuraminidase inhibitors themselves may inhibit bacterial neuraminidases, which could prove detrimental to the structure of the suspended biofilms that make up activated sludge. While this is yet to be fully investigated, current data indicate that the ecotoxicological risks posed by OC are low (Straub, 2009).

In addition to examining the potential evolution of OC degradation in a microbial consortium, we aimed to investigate the effects of OC and antibiotics on activated sludge bacterial community structure and function and activated sludge biofilm structure. We implemented a 56-day, pandemic-scenario dosing regime of OC and three antibiotics (with different modes of action): amoxicillin (cell-wall-synthesis inhibition), erythromycin (protein-synthesis inhibition) and levofloxacin (DNA-replication inhibition), in a laboratory-scale sequencing batch reactor (SBR) operated for granular enhanced biological phos-

phorus removal (EBPR). The three antibiotics selected for this study are among the most frequently used antibiotics, within their class, for the treatment of influenza-associated bacterial pneumonia (Lim *et al.*, 2007). An additional high-OC dosing period without antibiotics was used to examine OC toxicity and WWTP function in the absence of the presumed antibiotic stress.

Materials and methods

Reactor operation

A laboratory-scale SBR had a working volume of 8 L, with 2 L of treated wastewater removed and replaced with synthetic influent wastewater every 6 h, resulting in a HRT of 24 h. The sludge age was approximately 24 days. The synthetic influent wastewater contained either acetate or propionate as the sole carbon source (alternated on a fortnightly basis; Lu *et al.*, 2006) and orthophosphate (P-PO_4^{3-}) at concentrations of approximately 1100 mg chemical oxygen demand (COD) L^{-1} and 23 mg P-PO_4^{3-} L^{-1} , respectively (see Supporting Information for further details). The SBR was operated for EBPR, an activated sludge process for removing phosphate from wastewater. It is appropriate to investigate because it is commonly used in full-scale WWTPs and the bacterial community and biochemical transformations involved are well characterized (Seviour *et al.*, 2003). The current study used granular activated sludge as the reactor biomass. This is a novel activated sludge technology that selects for aggregates ($> 200 \mu\text{m}$) that are larger than those occurring in conventional floccular activated sludge (de Kreuk *et al.*, 2007).

The operational parameters necessary for EBPR include introducing the wastewater into an anaerobic phase of operation, with an aerobic phase following. Typically, during the anaerobic stage, the carbon source is taken up and phosphate is released by the bacteria, then in the subsequent aerobic phase the phosphate is taken up by the bacteria, over and above that which was released in the anaerobic phase (Seviour *et al.*, 2003). Before dosing of pharmaceuticals the SBR was performing good EBPR for more than 6 months. During dosing, the reactor operation did not change, except that the principal carbon source in the reactor feed was no longer alternated between acetate and propionate, but rather only acetate was used in order to reduce the number of variables. OC and antibiotics were added as detailed below.

OC and antibiotic dosing

The OC and antibiotic dosing for the SBR mirrored projected usage in the United Kingdom, as per A.C. Singer *et al.* (unpublished data), with a stepwise dosing up to the pandemic peak. OC and antibiotics were dissolved in sterile distilled water and added to autoclaved acetate feed. The

maximum amount of each antibiotic and OC in the reactor influent was: $36 \mu\text{g L}^{-1}$ OC, $70 \mu\text{g L}^{-1}$ amoxicillin, $30 \mu\text{g L}^{-1}$ erythromycin and $10 \mu\text{g L}^{-1}$ levofloxacin. During the 14-day OC-only dosing period, the reactor influent contained $360 \mu\text{g OC L}^{-1}$ (see Supporting Information, Table S1). At the peak of the simulated pandemic, the concentration of antibiotics and OC were ~ 2 to $20 \times$ projected mean concentrations in WWTPs as per A.C. Singer *et al.* (unpublished data), during a moderate pandemic ($R_0 = 2.3$, where R_0 indicates the average number of infections generated by an infectious individual in a fully susceptible population) with conservative estimates of Tamiflu[®] use within the populations (30% of infected people utilize OC). Although the experimental concentrations of pharmaceuticals in the reactor were above the mean projected levels (A.C. Singer *et al.*, unpublished data), they reflect a realistic worst-case scenario.

Measurement of OC

OC was quantified from the influent and effluent during a single cycle of the SBR on the final day of each dosing regime. Approximately 10 mL of each sample was filtered through a $0.22 \mu\text{m}$ disposable filter (Millipore, Billerica, MA) into glass GC vials and kept at -20°C until measurement. OC concentrations were measured by direct aqueous injection of the sample into an Agilent 6410B Triple Quad LC MS at the National Laboratory Services (Wales) (see Supporting Information for further details).

Biochemical analyses

Mixed liquor suspended solids (MLSS), effluent suspended solids (effluent SS) and mixed liquor volatile suspended solids (VSS) were measured according to standard methods (APHA, 1998). Ammonium (N-NH_4^+), nitrate (N-NO_3^-), nitrite (N-NO_2^-), orthophosphate (P-PO_4^{3-}) and acetate concentrations in the liquid phase were analysed at the AWMC Analytical Laboratory (Brisbane, Qld, Australia) (see Supporting Information for further details).

Granule structure analyses

Visual inspections of whole granules were performed using an Olympus SZH10 stereomicroscope with a DP70 digital camera. Approximately 25 mL of mixed liquor was removed from the SBR at the end of the aerobic phase and photographed in a glass Petri dish against a black background. Volumetric size distribution of granules was determined by pumping approximately 30 mL of mixed liquor (again, removed at the end of the aerobic phase) through a Malvern laser light-scattering instrument (Mastersizer 2000 series, Malvern 457 Instruments, Worcestershire, UK).

T-RFLP

T-RFLP analysis of 16S rRNA genes was carried out as described previously (Slater *et al.*, 2010) (see Supporting Information for further details).

FISH

Biomass samples were taken during the aerobic phase of the SBR and fixed in 4% paraformaldehyde in phosphate-buffered saline at 4°C for 2 h. FISH was performed as described previously (Amann, 1995) (see Supporting Information for further details).

Results

OC degradation

Over the experimental period, there was evidence of varying rates of removal of OC (Fig. 1). These were equivalent to between 2% and 41% removal per 6-h SBR cycle [estimated for each dosing period based on measured influent OC concentrations, four draw and fill cycles per day (Fig. S1) and assuming a constant rate of removal for each dosing period]. There was a general, although not consistent, trend for the removal rates to be lower in the latter part of the experiment (i.e. after day 35) than in the earlier part (Fig. 1).

Nutrient removal performance

Phosphate levels from full-scale WWTP effluents are legally regulated. The laboratory SBR was operating for biological phosphorus removal and thus this formed the basis for monitoring reactor function. Effluent P-PO_4^{3-} levels during the 40-day pre-pandemic simulation period and the first 21

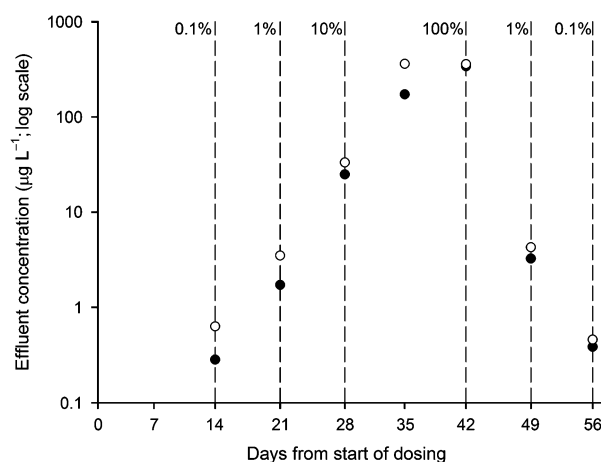


Fig. 1. Effluent OC concentration, showing observed values (filled circles) and predicted values assuming no degradation (open circles). Dotted lines represent the ends of a particular dosing regime and indicate the OC dosing level as a percentage of the maximum dose.

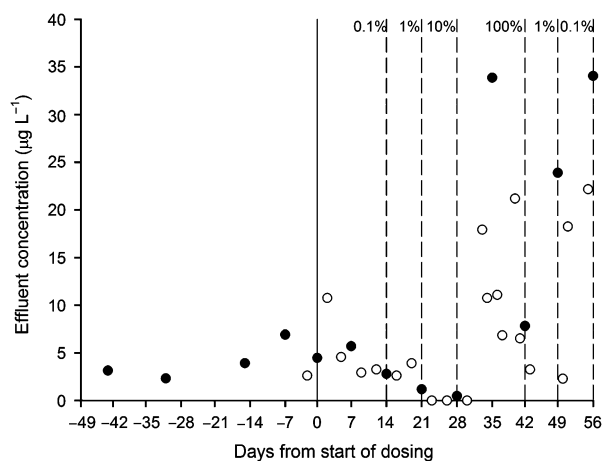


Fig. 2. Effluent P-PO_4^{3-} concentrations, from flow injection analysis (filled circles) and colourimetric tests (open circles). Dotted lines represent the ends of a particular dosing regime and indicate the OC dosing level as a percentage of the maximum dose.

days of the simulated pandemic (i.e. 0.1% and 1% OC dosing) were between 2 and 7 mg L^{-1} (Fig. 2). Notably, effluent P-PO_4^{3-} levels decreased to $< 1.2 \text{ mg L}^{-1}$ by day 28, indicating a well-functioning reactor. However, from day 33 at the beginning of the 100% OC-only dosing, effluent P-PO_4^{3-} values became erratic and were typically high, reaching a maximum of 34 mg L^{-1} , indicating reduced EBPR performance. This reduced EBPR during the dosing period was confirmed by other measures of performance. Firstly, the anaerobic phosphate release (Fig. S2; used by others previously as a measure of EBPR performance; Zilles *et al.*, 2002; He *et al.*, 2008; Slater *et al.*, 2010). Secondly, complete anaerobic consumption of acetate, which occurred for the 40-day prepandemic period and throughout the simulated pandemic period, failed on day 56, when consumption became incomplete (data not shown). Thirdly, nitrification (which occurred despite the operation of the SBR primarily for EBPR), as evidenced by aerobic nitrate production (Fig. S3), which decreased from over $0.85 \text{ mg N-NO}_3^- \text{ g}^{-1} \text{ VSS}$ for the prepandemic period and the first 35 days of simulated pandemic to below $0.4 \text{ mg N-NO}_3^- \text{ g}^{-1} \text{ VSS}$ at the end of the 100% OC dosing period.

Granule structure

The MLSS (equivalent to cell dry weight) in the SBR was between 12.68 and 15.12 g L^{-1} from 7 days before dosing to day 56 (data not shown). Granule particle size distribution was between approximately $80 \mu\text{m}$ (10th percentile) and $1320 \mu\text{m}$ (90th percentile), with a median granule size of approximately $620 \mu\text{m}$ (Fig. S4). Neither of these measures showed significant trends over the experiment. However, there were indications from light microscopy that some of

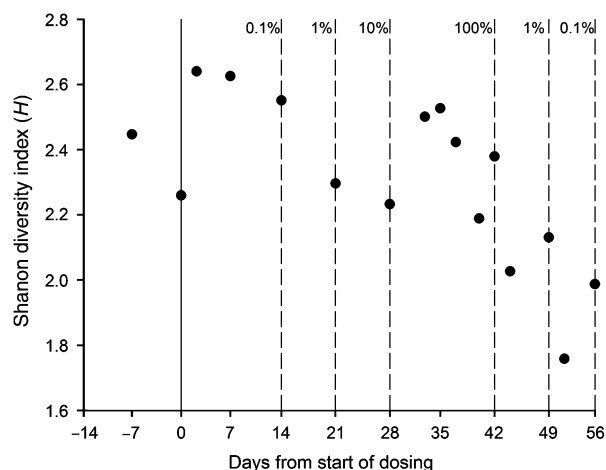


Fig. 3. Shannon diversity, H , derived from analysis of T-RFLP data. Dotted lines represent the ends of a particular dosing regime and indicate the OC dosing level as a percentage of the maximum dose.

the granules lost some structural integrity during the dosing as there was an appearance of fluffier material at days 49 and 58 (Fig. S5). Additionally, there was evidence of an increase in the effluent SS from approximately 100 mg L^{-1} before dosing to approximately 400 mg L^{-1} on days 42 and 56 (Fig. S6), suggesting that sludge settling was poorer due to granule biofilm disruption.

Bacterial community structure

The diversity indices derived from 16S rRNA T-RFLP data indicated that there were changes in the community structure over the dosing period, with the Shannon diversity index decreasing over the last 14 days of dosing (Fig. 3). This appeared to be a result of the development of a less even community structure (Fig. S7) rather than the disappearance of particular operational taxonomic units (Fig. S8). While there was therefore some evidence of a change in the diversity indices, i.e. those describing aggregate community characteristics, there appeared to be little change in the relative abundance of two of the model organisms commonly found in EBPR systems. The relative abundance of a key organism responsible for EBPR, *Candidatus 'Accumulibacter phosphatis'* (Hesselmann *et al.*, 1999), was 27.1% on day 0 (92% congruency score) and 22.8% on day 42 (end of 100% OC dosing; 96% congruency score), as assessed by quantitative FISH. The relative abundance of a glycogen-accumulating organism and known EBPR antagonist, *Candidatus 'Competibacter phosphatis'* (Crocetti *et al.*, 2002), was below 1% on days 0 and 42.

Discussion

This is the first study in which the removal of OC, microbial diversity, nutrient removal performance and granule

structure has been tested in a simulated activated sludge system exposed to OC and antibiotics in pandemic-scenario dosing.

There was up to 41% removal of OC per 6-h SBR cycle, with the most successful removal occurring in the first 35 days of dosing. It may be that in a real pandemic scenario, 35 days of significant removal at the beginning of an epidemic would reduce the amount of OC released into receiving waters. However, during the SBR operation, there was no evidence of significant OC removal after day 35. Hence, there does not appear to be sufficient selective pressure for the enrichment of OC degraders in the system investigated.

There was no evidence of any adverse effects on reactor performance during the first 28 days of the simulated pandemic (i.e. up to $36 \mu\text{g L}^{-1}$ OC, $70 \mu\text{g L}^{-1}$ amoxicillin, $30 \mu\text{g L}^{-1}$ erythromycin and $10 \mu\text{g L}^{-1}$ levofloxacin). There was, however, evidence during and after the two-week high-OC dosing period (days 29–42; $360 \mu\text{g L}^{-1}$ OC) of a reduction in EBPR and nitrification, bacterial community diversity and disruption to granule structure. This evidence of ecotoxicity in a simulated WWTP complements, but also contrasts with other studies that found no OC toxicity in freshwater (Accinelli *et al.*, 2010) and activated sludge performance (Straub, 2009; testing limited to COD removal only). The positioning of the high OC-only dosing period in the middle of the pandemic scenario (i.e. dosing of OC and antibiotics) meant that we were not able to completely differentiate the causes of the perturbation to community structure and function; however, it is clear from this study that WWTPs may experience reduced efficiency during an influenza pandemic owing to the high concentrations of bioactive pharmaceuticals, such as antivirals and antibiotics.

The SBR chosen for this study had a relatively long history of stable EBPR performance (> 6 months). EBPR failure has previously been shown to occur as a result of competition with glycogen-accumulating organisms (Bond *et al.*, 1999) and from bacteriophage infection (Barr *et al.*, 2010; Barr *et al.*, 2010); hence, the loss in reactor function in this study might not be due to pharmaceutical exposure. However, as quantitative FISH analyses did not demonstrate a decrease in the relative abundance of *Candidatus* 'Accumulibacter phosphatis', as would be expected if bacterial competition or bacteriophage predation was to blame, it was concluded that pharmaceutical exposure was the more likely cause. As the SBR was operated as a granular (rather than floccular) sludge, it remains untested whether floccular sludge would respond differently to such exposure. Granular sludge systems do have some operational differences to floccular systems, such as longer sludge ages, higher mixed liquor SS and lower available surface area, all of which might affect sludge–pharmaceutical interactions.

It was only after dosing high concentrations of antibiotics and OC that effects on EBPR performance were noticed.

Therefore, it may be that it is only under severe pandemic scenarios that disruption to WWTPs is of concern. Nonetheless, this research highlights the reality of this chemical risk to WWTP function and the need for additional mixed-pharmaceutical dosing studies in WWTP systems. These will be important for optimizing WWTP operation to contend with threats to WWTP function, and for understanding and modelling the release of pharmaceuticals into the environment.

Acknowledgements

We thank F. Hoffman-La Roche Ltd for the kind donation of OC and Michael Poole for assistance with Fig. S1. This work was funded by a UQ New Staff Research Start-up Grant awarded to F.R.S. and the Natural Environment Research Council – Knowledge Transfer Initiative (PRE-PARE) contract no. NE/F009216/1 awarded to A.C.S. We thank two anonymous reviewers for their comments on the text.

References

- Accinelli C, Caracciolo AB & Grenni P (2007) Degradation of the antiviral drug oseltamivir carboxylate in surface water samples. *Int J Environ An Ch* **87**: 579–587.
- Accinelli C, Sacca ML, Fick J, Mencarelli M, Lindberg R & Olsen B (2010) Dissipation and removal of oseltamivir (Tamiflu) in different aquatic environments. *Chemosphere* **79**: 891–897.
- Amann RI (1995) *In situ* identification of microorganisms by whole cell hybridization with rRNA-targeted nucleic acid probes. *Molecular Microbial Ecology Manual* (Akkerman ADL, Elsas DJV & Bruijn FJDOD, eds), pp. 1–15. Kluwer Academic Publishers, London.
- APHA (1998) *Standard Methods for the Examination of Water and Wastewater*. American Public Health Association, Washington, DC.
- Barr JJ, Slater FR, Fukushima T & Bond PL (2010) Evidence for bacteriophage activity causing community and performance changes in a phosphorus removal activated sludge. *FEMS Microbiol Ecol* **74**: 631–642.
- Bartels P & von Tumpling W (2008) The environmental fate of the antiviral drug oseltamivir carboxylate in different waters. *Sci Total Environ* **405**: 215–225.
- Bond PL, Erhart R, Wagner M, Keller J & Blackall LL (1999) Identification of some of the major groups of bacteria in efficient and nonefficient biological phosphorus removal activated sludge systems. *Appl Environ Microb* **65**: 4077–4084.
- Crocetti GR, Banfield JF, Keller J, Bond PL & Blackall LL (2002) Glycogen-accumulating organisms in laboratory-scale and full-scale wastewater treatment processes. *Microbiol-SGM* **148**: 3353–3364.
- Daughton CG & Ternes TA (1999) Pharmaceuticals and personal care products in the environment: agents of subtle change? *Environm Health Persp* **107**: 907–938.

- de Kreuk MK, Kishida N & van Loosdrecht MCM (2007) Aerobic granular sludge - state of the art. *Water Sci Technol* **55**: 75–81.
- Fick J, Lindberg R, Tysklind M, Haemig PD, Walderstrom J, Wallensten A & Olsen B (2007) Antiviral Oseltamivir is not removed or degraded in normal sewage water treatment: implications for development of resistance by Influenza A virus. *PLoS ONE* **2**: e986.
- Ghosh GC, Nakada N, Yamashita N & Tanaka H (2010) Oseltamivir carboxylate, the active metabolite of oseltamivir phosphate (Tamiflu), detected in sewage discharge and river water in Japan. *Environ Health Persp* **118**: 103–107.
- He G, Massarella J & Ward P (1999) Clinical pharmacokinetics of the prodrug oseltamivir and its active metabolite Ro 64-0802. *Clin Pharmacokinet* **37**: 471–484.
- He S, Gu AZ & McMahon KD (2008) Progress toward understanding the distribution of *Accumulibacter* among full-scale enhanced biological phosphorus removal systems. *Microb Ecol* **55**: 229–236.
- Hesselmann RPX, Werlen C, Hahn D, van der Meer JR & Zehnder AJB (1999) Enrichment, phylogenetic analysis and detection of a bacterium that performs enhanced biological phosphate removal in activated sludge. *Syst Appl Microbiol* **22**: 454–465.
- Lim WS, Douglas G, Honeybourne D *et al.* (2007) Pandemic flu: clinical management of patients with an influenza-like illness during an influenza pandemic. *Thorax* **62**: 1–46.
- Lu HB, Oehmen A, Virdis B, Keller J & Yuan ZG (2006) Obtaining highly enriched cultures of *Candidatus Accumulibacter phosphatis* through alternating carbon sources. *Water Res* **40**: 3838–3848.
- Parker D, Soong G, Planet P, Brower J, Ratner AJ & Prince A (2009) The NanA neuraminidase of *Streptococcus pneumoniae* is involved in biofilm formation. *Infect Immun* **77**: 3722–3730.
- Prasse C, Schlusener MP, Schulz R & Ternes TA (2010) Antiviral drugs in wastewater and surface waters: a new pharmaceutical class of environmental relevance? *Environ Sci Technol* **44**: 1728–1735.
- Sacca ML, Accinelli C, Fick J, Lindberg R & Olsen B (2009) Environmental fate of the antiviral drug Tamiflu in two aquatic ecosystems. *Chemosphere* **75**: 28–33.
- Seviour RJ, Mino T & Onuki M (2003) The microbiology of biological phosphorus removal in activated sludge systems. *FEMS Microbiol Rev* **27**: 99–127.
- Singer AC, Nunn MA, Gould EA & Johnson AC (2007) Potential risks associated with the proposed widespread use of Tamiflu. *Environ Health Persp* **115**: 102–106.
- Singer AC, Johnson AC, Anderson PD & Snyder SA (2008) Reassessing the risks of Tamiflu use during a pandemic to the Lower Colorado River. *Environ Health Persp* **116**: A285–A286.
- Slater FR, Johnson CR, Blackall LL, Beiko RG & Bond PL (2010) Monitoring associations between clade-level variation, overall community structure and ecosystem function in enhanced biological phosphorus removal (EBPR) systems using terminal-restriction fragment length polymorphism (T-RFLP). *Water Res* **44**: 4908–4923.
- Soderstrom H, Jarhult JD, Fick J, Lindberg R, Singer AC, Grabic R & Olsen B (2010) Levels of antivirals and antibiotics in the river Thames, UK, during the pandemic 2009. *SETAC Europe Annual Meeting, Seville*.
- Soong G, Muir A, Gomez MI *et al.* (2006) Bacterial neuraminidase facilitates mucosal infection by participating in biofilm production. *J Clin Invest* **116**: 2297–2305.
- Straub JO (2009) An environmental risk assessment for oseltamivir (Tamiflu®) for sewage works and surface waters under seasonal-influenza- and pandemic-use conditions. *Ecotoxicol Environ Saf* **72**: 1625–1634.
- Zilles JL, Peccia J, Kim MW, Hung CH & Noguera DR (2002) Involvement of *Rhodocyclus*-related organisms in phosphorus removal in full-scale wastewater treatment plants. *Appl Environ Microb* **68**: 2763–2769.

Supporting information

Additional Supporting Information may be found in the online version of this article:

Fig. S1. Simulated effluent OC concentrations based on measured influent OC concentrations and four SBR draw and fill occurrences per day, each with a volumetric exchange ratio of 1:4, and assuming no sorption or biological transformation (i.e. no removal of OC) by sludge.

Fig. S2. Anaerobic P-PO₄⁻³ release (normalized to VSS; analogous to cell dry weight).

Fig. S3. Aerobic nitrate production (normalized to VSS; analogous to cell dry weight).

Fig. S4. Particle size distribution of granules, including 10th (filled circles), 50th (open circles) and 90th (filled triangles) percentiles.

Fig. S4. Particle size distribution of granules, including 10th (filled circles), 50th (open circles) and 90th (filled triangles) percentiles.

Fig. S5. Light microscopy images of granules against a black background taken on different days at different dosing regimes (indicated as the OC dosing level as a percentage of the maximum dose).

Fig. S6. Effluent SS.

Fig. S7. Shannon evenness (*J*) derived from T-RFLP data.

Fig. S8. Richness (*S*) derived from T-RFLP data.

Table S1. Dosing of pharmaceuticals.

Appendix S1. Reactor operation.

Please note: Wiley-Blackwell is not responsible for the content or functionality of any supporting materials supplied by the authors. Any queries (other than missing material) should be directed to the corresponding author for the article.